INSTITUTE FOR NUCLEAR STUDY
UNIVERSITY OF TOKYO
Tanashi, Tokyo 188
Japan

INS-Rep.-650
Sept. 1987

SPECTROSCOPY OF HYPERNUCLEI WITH STOPPED KAONS — RECENT RESULT OF KEK EXPERIMENT

H. Tamura, W. Brückner, H. Döbbeling, R.S. Hayano, T. Ishikawa, M. Iwasaki, T. Motoki, H. Outa, S. Paul, B. Povh, A. Sakaguchi, R. Schüssler, E. Takada, K.-H. Tanaka and T. Yamazaki

INS-Rep.-650
Sept. 1987

SPECTROSCOPY OF HYPERNUCLEI WITH STOPPED KAONS — RECENT RESULT OF KEK EXPERIMENT

H. Tamura, W. Brückner***, H. Döbbeling***, R.S. Hayano*, T. Ishikawa*, M. Iwasaki*, T. Motoki*, H. Outa*, S. Paul***, B. Povh***, A. Sakaguchi***, R. Schüssler***, E. Takada*, K.-H. Tanaka** and T. Yamazaki

Institute for Nuclear Study, University of Tokyo, Tanashi, Japan
* Department of Physics, Faculty of Science, University of Tokyo, Tokyo, Japan
** National Laboratory for High Energy Physics (KEK), Tsukuba, Ibaraki, Japan
*** Max Planck Institut für Kernphysik, Heidelberg, F.R.Germany

Pion momentum spectra from K^- absorption at rest on various nuclear targets were measured by means of a magnetic spectrometer with wide momentum range (100 ~ 300 MeV/c). The ground state of Σ^- hypernucleus, if well bound with a narrow width, is expected to be populated in ^{12}C(stopped K^-,π^+) inclusive (untagged) spectrum, but such a peak was not observed. The spectrum is compared with the DWIA calculations by Morimatsu and Yazaki, indicating that the depth of the nuclear potential of Σ^- is shallower than 12 MeV, and that its imaginary part is larger than 5 MeV if the potential depth is about 10 MeV. In the ^{12}C(stopped K^-,π^-) spectrum, the ground state $((p3/2)_n^{-1}\ (s1/2)_\Lambda)$ and the excited states $((p3/2)_n^{-1}(p)_\Lambda)$ of $^{12}_{\Lambda}$C were observed, and their formation probabilities were roughly in agreement with the results of DWIA calculations. In the π^- spectra on ^{12}C, ^{9}Be, and ^{7}Li targets a distinct peak was observed at 132.1±0.7 MeV/c. It is ascribed to π^- from the mesic decay of $^{4}_{\Lambda}$H; $^{4}_{\Lambda}\mathrm{H} \rightarrow {}^{4}\mathrm{He}\ \pi^-$. The formation probability of $^{4}_{\Lambda}$H on C, Be, or Li target is much larger than those of the discrete states of $^{12}_{\Lambda}$C via the direct (stopped K^-,π^-) reaction.

1. INTRODUCTION

Spectroscopy of hypernuclei with stopped K^- has been discussed and pursued in these several years. It was pointed out that a large formation probability of Σ hypernuclei in the K^- absorption at rest enables Σ hypernuclear spectroscopy with high statistical quality [1], which is not easily achieved in the in-flight (K^-,π) reactions. Thanks to its larger momentum transfer (170 MeV/c for Σ and 250 MeV/c for Λ), moreover, the stopped K^- reaction is expected to be suitable for the population of non-substitutional hypernuclear states, such as a ground state or spin-orbit doublets.

Since the first observation of narrow Σ hypernuclear states [2], several narrow states have been reported with the in-flight (K^-,π) reaction [3,4,5] and they have brought about an interesting puzzle why such a narrow width is realized in spite of the strong Σ-Λ conversion in a nucleus. In order to understand the mechanism of the suppression of the conversion, it should be most crucial to see whether the ground state exists with a narrow width or not. These in-flight experiments were, however, not fitted to populate the ground state, while the stopped K^- experiment was expected to be promising. Probabilities of Σ hypernucleus population by (stopped K^-, π^+) were calculated based on the bound state approximation [6,7], and recently

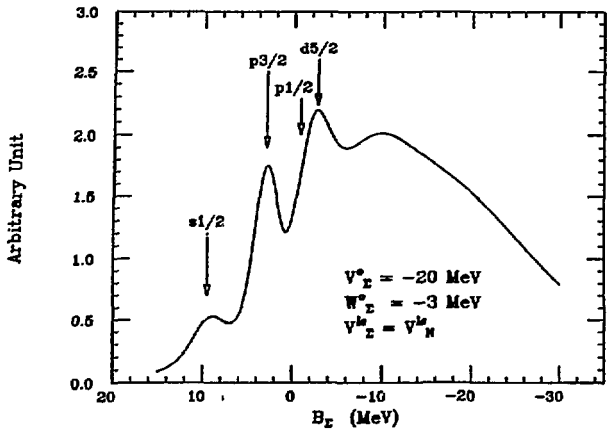

FIGURE 1
^{12}C(stopped K^-,π^+) spectrum predicted by Morimatsu and Yazaki's calculation with a set of typical potential parameters. An experimental resolution (2 MeV FWHM) is folded.

Morimatsu and Yazaki introduced a calculation with a strongly absorptive potential, which can treat the unbound continuum states realistically by the Green-function method [8]. Their calculation predicted a spectrum like Fig.1, assuming the hitherto believed single-particle potential (20 MeV deep with a small Σ-Λ conversion).

In 1983, the Tokyo group measured a ^{12}C(stopped K^-,π^+) spectrum on an active scintillator target as a byproduct of the study of $K^+ \to \mu\nu$ decay. They observed narrow Σ^- hypernuclear peaks in the spectrum in coincidence with π^0 [9]. The ground state region was, however, disturbed by a background peak from hydrogen in the scintillator target. Therefore, the use of hydrogen-free targets was required for further studies.

Since 1986, we have performed a series of dedicated experiments to study Σ and Λ hypernuclei using stopped K^- at KEK. The main purpose for these experiments was to search for the ground states of Σ hypernuclei as well as to confirm the previous result with the narrow peaks in the unbound region.

We also hoped that the stopped K^- reaction provides us with new information on Λ hypernuclei. In this paper we will report recent results of these new experiments.

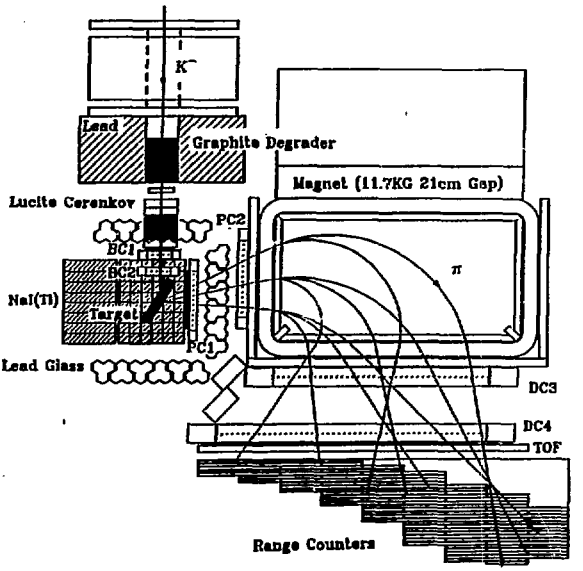

FIGURE 2
Schematic figure of the experimental setup (top view).

2. EXPERIMENTAL SETUP AND DETECTOR PERFORMANCES

The experiments were carried out at the K3 beamline of KEK 12GeV PS. The experimental setup is illustrated in Fig.2. A detailed description can be found in Ref.10.

Negative kaons were separated by a DC mass-separator, degraded in graphite, and stopped in a thick (about 10g/cm^2) target. The beam momentum was chosen to be 650 MeV/c, which is optimum for stopped K^- yield taking into account the decay loss and the beam spread after the degradation. We obtained 3×10^3 stopped K^-'s per spill for a primary beam of 2.0×10^{12} protons. Three Lucite Čerenkov counters were used to reject pions.

Momenta of pions emitted from the target were measured with a spectrometer magnet (C-type, 11.7 kG) and a set of four tracking chambers (2 MWPC's and 2 drift chambers; each of them has a cathode readout). This spectrometer system has a high momentum resolution ($\Delta p \sim 1.0$ MeV/c FWHM) and a large acceptance (~100 msr). The spectrometer covers a wide momentum range from 100 MeV/c to 300 MeV/c, which enables us to study both of Σ and Λ hypernuclei simultaneously as shown in Fig.3. With this system, moreover, we can

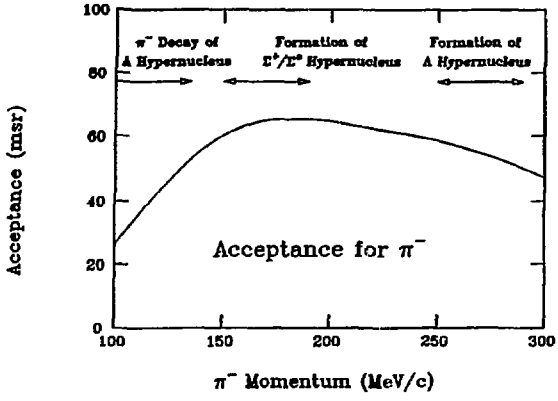

FIGURE 3

Acceptance of the spectrometer as a function of the π^- momentum (calculated by a Monte Carlo simulation). The loss of pions due to the decay in-flight and the reaction in the target are taken into account. Regions for different hypernuclear studies are shown.

observe mesonic decays of Λ hypernuclei which appear around 100 MeV/c in π^- spectra.

Since we need to use a thick target to gain the stopped K^- yield, the energy loss of pions in the target should be corrected for. We measured reaction points in the target by using two MWPC's (BC1,BC2) just before the target along the K^- beam and two MWPC's (PC1,PC2) at the entrance of the spectrometer magnet. The spatial resolution of the reaction points is 6 mm FWHM, which is mainly determined by multiple scattering of K^- in the target. The absolute momentum scale was checked by use of several monochromatic peaks; $K^+ \rightarrow \mu^+\nu$ (235.5 MeV/c), $K^+ \rightarrow \pi^+\pi^0$ (205.1 MeV/c), $\Sigma^+ \rightarrow \pi^+ n$ (185.0 MeV/c), and $K^-p \rightarrow \Sigma^-\pi^+$ (172.9 MeV/c). The widths of these peaks and the observed hypernuclear peak of $^{12}_{\Lambda}C$ (261 MeV/c and 273 MeV/c) were 2.0~2.7 MeV/c, and that of $^{4}_{\Lambda}H \rightarrow {}^{4}He\ \pi^-$ peak (133 MeV/c) was 3.4 MeV/c. Therefore the momentum resolution of 2.0~3.4 MeV/c (FWHM) was achieved over the full momentum range. For the hypernuclear mass, a 1.7~2.5 MeV (FWHM) resolution was obtained, which slightly depended on the target material.

The ranges of particles coming through the spectrometer were measured by a stack of scintillation counters (Range Counters), by which pions were discriminated from muons. In the (K^-,π^+) mode, we used a time-of-flight between B2 and TOF counters and rejected protons.

The target was surrounded by NaI counters and lead glass counters with plastic scintillation counters in front of them. These counters were used to detect π^0, $\pi^\pm$, protons, and γ rays which may be emitted in the formation and the decay of hypernuclei.

Table 1. Summary of the (stopped K^-,π) experiments at KEK.

Target	Reaction Mode	Number of Pion Events
$(CH)_n$ (scintillator)	(K^-, π^+)	2.2×10^5
$(CH)_n$ (scintillator)	(K^-, π^-)	4.0×10^5
C (graphite)	(K^-, π^+)	7.8×10^4
C (graphite)	(K^-, π^-)	4.7×10^4
Be	(K^-, π^-)	3.8×10^5
Li	(K^-, π^-)	2.0×10^5

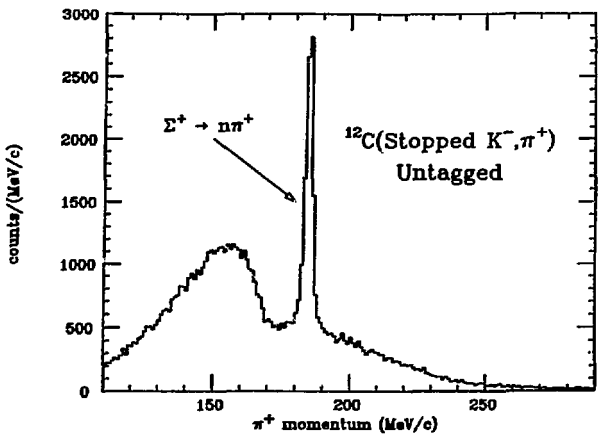

FIGURE 4
Inclusive ("untagged") (stopped K^-, π^+) spectrum on ^{12}C (graphite) target. Acceptance is corrected for.

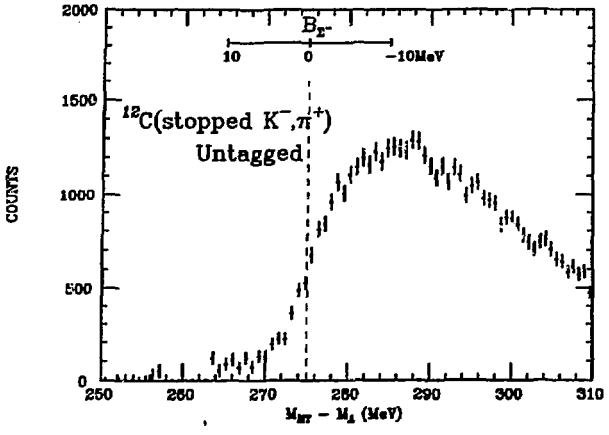

FIGURE 5
Inclusive ^{12}C (stopped K$^-$,π^+) spectrum in the energy scale after the background subtraction.

Data-taking was performed with VAX-11/750 via CAMAC system. The trigger rate was about 5 for the (K$^-$,π^+) mode and about 10 per spill for the (K$^-$,π^-) mode . In Table 1, targets, reaction modes, and numbers of accumulated pion events are summarized.

3. ^{12}C(STOPPED K$^-$,π^+) SPECTRUM AND Σ HYPERNUCLEUS

We measured (stopped K$^-$, π^+) spectra with high statistical quality on the scintillator and the graphite target. The graphite target was used to study the ground state of Σ hypernucleus, because hydrogen in the scintillator target causes a peak from K$^-$p→Σ$^-\pi^+$ in the momentum region where the Σ hypernuclear ground state is expected.

Here we will concentrate on the "untagged", i.e., inclusive spectrum on the graphite target. This untagged spectrum is unbiased and suitable for comparison with theoretical calculations.

3.1 ^{12}C(Stopped K$^-$,π^+) Spectrum

Fig.4 shows the untagged (stopped K$^-$, π^+) spectrum on the graphite target. The spectrum consists of two parts; (1) the peak at 185MeV/c and the tails on both sides, which come from Σ$^+$→π^+n decay at rest and in-flight, respectively, and (2) the broad bump below 170 MeV/c due to the Σ$^-$ production on a ^{12}C nucleus. The background hydrogen peak at 173 MeV/c disappeared.

The Σ$^+$ decay background was subtracted from the spectrum. Here, the tail component of the low momentum side of the 185 MeV/c peak can be reliably subtracted with reference to

the shape of the higher momentum side. The contribution of other backgrounds resulting from in-flight $K^- \to \pi^+\pi^-\pi^-$ decay and in-flight (K^-,π^+) reaction before K^- stops in the target were estimated to be negligible. In Fig.5 we plotted the background-subtracted spectrum in the energy scale $M_{HY} - M_A$, where M_{HY} is the hypernuclear mass and M_A is the target nuclear mass.

It is remarkable that the narrow Σ^- hypernuclear bound states expected as in Fig.1 are not seen. This fact sets a constraint on the Σ^- potential, as discussed later.

3.2 Discussions of the Nuclear Potential of Σ

Recenly, DWIA calculations of (stopped K^-, π^+) spectrum became available by Morimatsu and Yazaki [8] and by Kohno *et al* [12], in which the unbound continuum region can be calculated with the conversion process taken into account. Here we discuss the nuclear potential of Σ by comparing the spectrum with the calculation by Morimatsu and Yazaki. A detailed discussion is reported in Ref.11.

In the calculation by Morimatsu-Yazaki, an optical potential

$$U_\Sigma(r) = (V_\Sigma^0 + iW_\Sigma^0)\rho(r)/\rho_0$$

was used for Σ, where $\rho(r)$ has the Woods-Saxon form with $r_0 = 1.27A^{1/3}$ and $a = 0.67$ fm, and the nuclear mass density $\rho_0 = 0.17$ fm^{-3}. The imaginary part represents the Σ-Λ conversion process. Namely, the imaginary part is related to the conversion width Γ_c as $\Gamma_c = 2|\overline{W_\Sigma}|$, where $|\overline{W_\Sigma}|$ is the imagenary part averaged over the hyperon density. Here the spreading width is not considered explicitly.

According to the calculation (see Fig.1), the untagged (stopped K^-,π^+) spectrum should reveal peaks for the ground state and the excited states, if the conversion width is small ($W_\Sigma^0 = -3$ MeV) and the central potential is deep enough ($V_\Sigma^0 = -15$ MeV). Spectra were calculated with various parameter sets (V_Σ^0, W_Σ^0) and compared with the data. In Fig.6, for example, calculated spectra with a small W_Σ^0 ($= -3$ MeV) and various V_Σ^0 are shown together with the data.

The following constraints for the parameters were derived.

(1) $|V_\Sigma^0| < 12$ MeV. If V_Σ^0 is deeper, the spectrum should have an excessive strength in the bound region ($B_\Sigma > 0$).

(2) $|W_\Sigma^0| > 6$ MeV for $|V_\Sigma^0| \approx 10$ MeV. If $|W_\Sigma^0|$ is smaller, the ground state peak would be visible.

(3) The spectrum is insensitive to $|W_\Sigma^0|$, when $|V_\Sigma^0| < 5$ MeV. Accordingly, if $|W_\Sigma^0|$ is as small as suggested in the experiments so far, then $|V_\Sigma^0|$ should be smaller than 5 MeV.

(4) A large spin-orbit splitting ($|V_\Sigma^{ls}| \geq 2|V_N^{ls}|$), is not favoured. If $|V_\Sigma^{ls}|$ is so large, an excessive strength (or a peak) would be seen in the bound region due to the contribution of the lower state of the spin-orbit doublet $(p3/2 + p1/2)_\Sigma$. Only when $|V_\Sigma^0| < 5$ MeV, the data are insensitive to $|V_\Sigma^{ls}|$.

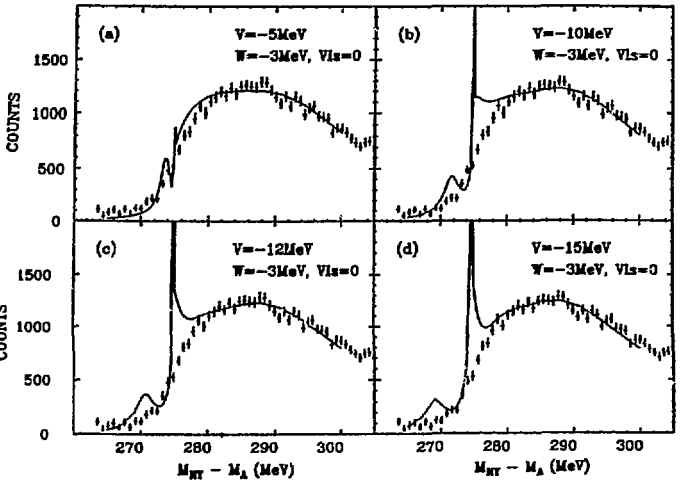

FIGURE 6

Comparison between the data and the calculation for ^{12}C (stopped K^-,π^+) spectrum. The data (Fig.5) are plotted in dots, and results of DWIA calculation with various Σ potential parameters are shown in solid lines.

The present data are not inconsistent with the potential parameters determined by Σ^- atomic X-ray data ($|V_\Sigma^0| \approx 10$ MeV and $|W_\Sigma^0| \approx 9$ MeV) (see Ref.11).

As shown in the above discussions, the untagged spectrum does not favour the small (less than 4 MeV) conversion width reported by the previous experiments [4,5,9]. It should be noted, however, that the discussion is within the framework of the single-particle model for Σ^-.

4. ^{12}C (Stopped K^-,π^-) SPECTRUM AND Λ HYPERNUCLEI

In this section we will discuss Λ hypernuclei using (stopped K^-,π^-) spectrum on carbon (scintillator) target.

4.1 Spectrum and Background

Fig.7 shows π^- momentum spectrum on the scintillator target. The global structure of the spectrum can be understood with productions and decays of hyperons as follows.

The histograms drawn in Fig.7 show Monte-Carlo simulated spectra of (a) quasi-free Σ^+ production ($K^-p \rightarrow \Sigma^+\pi^-$), (b) quasi-free Λ production ($K^-n \rightarrow \Lambda\pi^-$), (c) Σ^- decay ($\Sigma^- \rightarrow n\pi^-$), and (d) Λ decay ($\Lambda \rightarrow p\pi^-$). Here we neglected the quasi-free Σ^0 production ($K^-n \rightarrow$

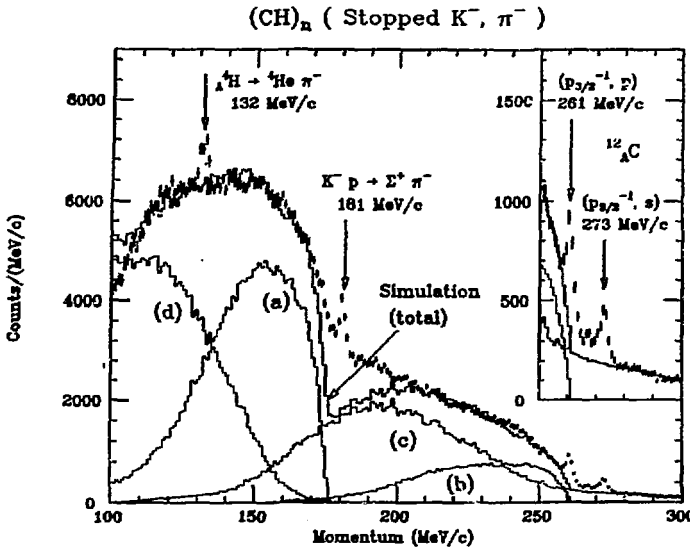

FIGURE 7
Inclusive (stopped K^-, π^-) spectrum on ^{12}C (dots) with the expected spectrum calculated by Monte Carlo simulation (histogram). (a), (b), (c), and (d) show the contributions of the individual processes (see text). Acceptance is corrected for.

$\Sigma^0\pi^-$), since its intensity is known to be 10% of that of the Σ^+ production [13]. The simulation took into account Fermi-motion of nucleons and energy loss of hyperons in the target. The relative intensity of each component was determined so that the summed spectrum reproduces the data. The spectrum can be explained qualitatively.

Around the threshold of Λ binding, two peaks were observed at 260.9 ± 0.3 MeV/c and at 272.8 ± 0.5 MeV/c. Fig.8(c) is the same spectrum plotted in the scale of $M_{HY} - M_\Lambda$ and B_Λ. The two peaks correspond to the $(p3/2)_n^{-1}(p)_\Lambda$ (B_Λ= 0 MeV) states and the $(p3/2)_n^{-1}(s)_\Lambda$ state (ground state, B_Λ= 11 MeV) of $^{12}_\Lambda C$ which were found in several experiments [14,15,16]. The previous $^{12}_\Lambda C$ spectra by the in-flight (K^-,π^-) reaction [15] and by the (stopped K^-, π^-) reaction [14] are shown together in Fig.8(a) and (b), respectively.

In the stopped K^- reaction, the peak at B_Λ = 0 MeV consists of the three states,

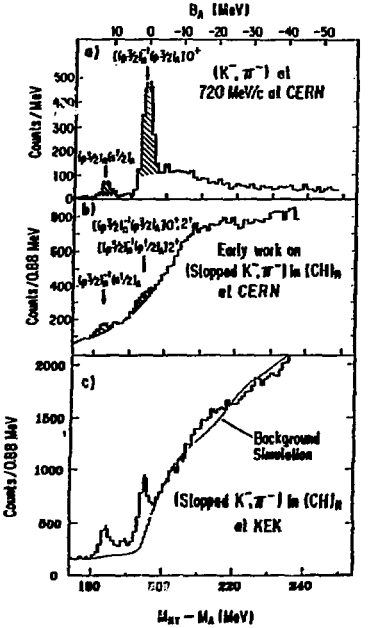

FIGURE 8

Fig. c) shows Λ hypernuclear region of ^{12}C(stopped K$^-$,π$^-$) spectrum in the energy scale. Fig. a) and b) are the previous data by in-flight [15] and by stopped [14] (K$^-$,π$^-$) reactions on ^{12}C.

$(p3/2)_n^{-1}(p3/2)_\Lambda$ [0$^+$,2$^+$] and $(p3/2)_n^{-1}(p1/2)_\Lambda$ [2$^+$]. According to the emulsion experiments with stopped K$^-$ [16], these three excited states are located just below the Λ binding threshold.

4.2 Formation Probabilities of $^{12}_{\Lambda}$C

The Λ hypernuclear region of the spectrum (Fig.8(c)) was fitted with two gaussian peaks and a background, and $^{12}_{\Lambda}$C formation probabilities were extracted.

The intensities of the peaks depend on the way how to draw a background. The simulated background shown in Fig.8(c) (Λ quasi-free and Σ$^-$ decay) does not fit the data exactly and leaves excess of events between the two peaks. The possible reasons are as follows. 1) The shape of the quasi-free background near the threshold is deformed due to final state interactions. 2) Other hypernuclear states with core (^{11}C) excitations should exist besides the prominent

Table 2. $^{12}_{\Lambda}$C formation probability by (stopped K^-,π^-) from the new KEK experiment and from the old CERN experiment [14]. Theoretical calculations are taken from Ref.6 and Ref.7.

	$P(j_N^{-1}, j_Y[J])$		
	$(s1/2)_\Lambda$ [1^-]	$(p3/2+p1/2)_\Lambda$ [0^++2^+]	$p[0^+$+$2^+)/s[1^-]$
This Experiment	$0.60\pm0.19 \times 10^{-3}$	$1.1\pm0.4 \times 10^{-3}$	1.8±0.8
Exp. Faessler	$0.2\pm0.1 \times 10^{-3}$	$0.3\pm0.1 \times 10^{-3}$	1.5±0.9
Calc. Matsuyama	0.12×10^{-3}	0.59×10^{-3}	4.9
Calc. Gal (b)	0.33×10^{-3}	0.96×10^{-3}	2.9

two peaks. The ambiguity of the peak intensities were estimated by applying two ways to draw the background; (1) smooth background with a polynomial function, and (2) the simulated background.

Experimentally, the hypernuclear formation ratio per $\Lambda\pi^-$ process, $R(j_N^{-1}, j_Y[J])$, can be obtained as the ratio of the peak intensity to the quasi-free Λ (Fig.7 histogram (b)) intensity. The intensity of the quasi-free Λ may have an ambiguity from the simulation, because this quasi-free Λ spectrum was calculated without considering the distortion of pion and hyperon wavefunctions in a nucleus, and fitted to the data.

The DWIA calculations of the $^{12}_{\Lambda}$C formation with stopped K^- were performed by Matsuyama-Yazaki [6] and by Gal-Klieb [7]. In the calculation by Matsuyama-Yazaki, the formation ratio $R(j_N^{-1}, j_Y[J])$, was calculated from :

$$\frac{\int d\Omega_k \left| \sum_{m,m_N,m_Y} \int d\vec{r}\, (j_Y m_Y j_N m_N | JM) \chi_\pi^{(-)*}(\vec{k},\vec{r}) \phi^*_{j_Y m_Y}(\vec{r}) \phi_{j_N m_N}(\vec{r}) \psi_{nlm}(\vec{r}) \right|^2}{\int d\vec{k} \sum_m \int d\vec{r}\, |\chi_\pi^{(-)}(\vec{k},\vec{r})|^2 \rho_N(\vec{r}) |\psi_{nlm}(\vec{r})|^2}$$

where $\chi_\pi(\vec{k},\vec{r})$ is the distorted wave function of the outgoing pion, ψ_{nlm} is the wave function of the kaonic atom when K^- is absorbed, $\phi_{j_N m_N}$ and $\phi_{j_Y m_Y}$ are the wave functions of the initial nucleon state and of the final hyperon state, respectively, and ρ_N is the initial nucleon density. The central potential depth of 30 MeV and zero spin-orbit splitting are assumed for Λ.

In this calculation, the above formation ratio was converted to "probability per stopped K^-" by :

$$P(j_N^{-1}, j_Y[J]) = R(j_N^{-1}, j_Y[J])\ \overline{A_\pi}\ BR(\Lambda\pi^-),$$

where $\overline{A_\pi}$ (=0.464 for $\Lambda\pi^-$) is the probability that the pion is not absorbed in the nucleus, and $BR(\Lambda\pi^-)$ (= 0.07; from an experiment [13]) is the branching ratio of $\Lambda\pi^-$ per stopped K^-.

Our experimental values of $R(j_N^{-1}, j_Y[J])$ were converted to the probabilities per stopped K^- $P(j_N^{-1}, j_Y[J])$ by use of the above equation. For the factor $\overline{A_\pi}\ BR(\Lambda\pi^-)$, we used the same value as in the calculation (0.032) to allow a straightforward comparison between the experiment

Table 3. $^{4}_{\Lambda}H$ formation probabilities formed by stopped K^- on $(CH)_n$, Be, and Li targets. $^{4}_{\Lambda}H \rightarrow {}^{4}He\ \pi^-$ decay branching ratio is assumed to be 0.7.

Target	Probability per Stopped K^-
Li	$6\pm2 \times 10^{-3}$
Be	$3.6\pm1.4 \times 10^{-3}$
$(CH)_n$	$3.4\pm1.0 \times 10^{-3}$

and the calculation. The experimental value of the factor was $\overline{A_\pi}\ BR(\Lambda\pi^-) = 0.04\pm0.01$ (preliminary), which is consistent with the above value. The results are listed in Table 2, where the errors include statistical ones and the ambiguity of the background subtraction, but do not include a normalization error from the quasi-free Λ intensity.

The calculated values of $P(j_N^{-1},j_Y[J])$ (probabilities per stopped K^-) by Matsuyama and Yazaki [6] and by Gal and Kfieb [7] are also listed in Table 2. It shows that the calculations are roughly in agreement with the experiment. It is noticeable, however, that the ratio of the p-state $[0^+ + 2^+ + 2^+]$ probability to the s-state $[1^-]$ probability in the experiment, which is free from the ambiguity of the normalization, is significantly smaller than that in the calculations.

5. FORMATION OF $^{4}_{\Lambda}H$ HYPERNUCLEUS

In the (stopped K^-,π^-) spectra on the carbon, beryllium, and lithium targets, a distinct peak was observed at 132.1±0.7 MeV/c. It is ascribed to π^- from the two-body mesonic decay of $^{4}_{\Lambda}H$; $^{4}_{\Lambda}H \rightarrow {}^{4}He\ \pi^-$ ($p_{\pi^-} = 132.9$ MeV/c, adopting 2.04 MeV as a binding energy of Λ in $^{4}_{\Lambda}H$ [17]).

The formation probability of $^{4}_{\Lambda}H$ was obtained from the peak intensity as listed in Table 3, assuming a branching ratio of $^{4}_{\Lambda}H \rightarrow {}^{4}He\ \pi^-$ decay to be 0.7 (see Appendix). The errors in the table are mainly due to the ambiguity of the normalization. The result indicates that the formation probability of $^{4}_{\Lambda}H$ is much larger than those of discrete states of $^{12}_{\Lambda}C$, which are formed via the direct (K^-,π^-) reaction. $^{4}_{\Lambda}H$ is presumably formed by multi-step reactions, or via a compound nucleus with Λ and its successive particle evaporation.

Table 4 shows the π^- decays of light hyperfragments observed in the old emulsion experiments, where numbers of events for the two-body decay modes are summarized (taken from Ref.18), together with expected π^- momenta from the two-body decays. Our observation is consistent with the fact that the two-body π^- decays of $^{4}_{\Lambda}H$ had the largest numbers of events among the observed two-body π^- decays of hyperfragments in Table 4.

6. NEW POSSIBILITY OF HYPERNUCLEAR STUDY WITH STOPPED K^-

The present result of the large formation probability of $^{4}_{\Lambda}H$ implies that much more hyper-

Table 4. π^- decays of light Λ hypernuclei. Numbers of observed events for the two body π^- decay and for other π^- decays are taken from Ref.18. Momenta and Q-values of the 2 body decays are calculated from the Λ binding energies in Ref.17.

Hypernuclei	*Number of π^- Decay Events*			*Q value*	*P_π (2 body)*
	2 body		others	(MeV)	(MeV/c)
${}^{3}_{\Lambda}$H	π^- ^{3}He	112	22	43.1	114.2
${}^{4}_{\Lambda}$H	π^- ^{4}He	760	93	55.5	132.9
${}^{4}_{\Lambda}$He	-	-	179	-	-
${}^{5}_{\Lambda}$He	-	-	1025	-	-
${}^{6}_{\Lambda}$He	π^- ^{6}Li	0	11	38.1	108.2
${}^{7}_{\Lambda}$Li	π^- ^{7}Be	3	64	37.8	108.0
${}^{7}_{\Lambda}$Be	-	-	10	-	-
${}^{8}_{\Lambda}$Li	π^- ^{8}Be	0	229	48.2	124.1
${}^{8}_{\Lambda}$Be	π^- ^{8}B	17	12	31.0	97.0
${}^{9}_{\Lambda}$Li	π^- ^{9}Be	5	9	46.1	121.1
${}^{9}_{\Lambda}$Be	π^- ^{9}B(g.s)	159	16	30.9	96.8
${}^{11}_{\Lambda}$B	π^- ^{11}C	4	7	36.2	105.9
${}^{12}_{\Lambda}$B	π^- ^{12}C	0	24	42.3	115.7
${}^{13}_{\Lambda}$C	π^- ^{13}N	1	0	28.5	92.9

nuclei (hyperfragments) are produced by stopped K^- through indirect processes than through the direct (stopped K^-,π^-) reaction.

The hypernuclear ground states, formed via indirect processes by stopped K^-, can be easily identified by their two-body π^- decay, if its branching ratio is not very small. If we measure nuclear γ rays together with π^- momentum, low lying states of a certain Λ hypernucleus, especially a spin-spin doublet of its ground state, can be studied by tagging the γ ray spectrum by the corresponding π^- peak. The superconducting toroidal spectrometer with a large acceptance (11% × 4π sr), which is being built by the Tokyo group, and high resolution photon detectors will be suitable for such experiments.

Taking advantage of stopped K^- as the efficient source of Λ hypernuclei, the lifetimes of heavy Λ hypernuclei (hyperfragments) can be measured by use of stopped K^- [19]. It is worthwhile to measure the averaged lifetimes of hypernuclei formed by stopped K^- on a heavy nuclear target, even though individual hypernuclear species are not distinguished.

ACKNOWLEDGEMENT

We would like to thank Professor K.Yazaki and Professor H.Bando for the discussions with their theoretical works. We are also grateful to Professors T. Nishikawa, H. Sugawara, H. Hirabayashi, K. Nakai, and the operating crew of the KEK PS and the beamlines for the support of the experiments.

APPENDIX: Branching Ratio of ${}^{4}_{\Lambda}\mathrm{H} \rightarrow {}^{4}\mathrm{He}\ \pi^-$

Concerning the partial decay rates of ${}^{4}_{\Lambda}\mathrm{H}$, the followings are known:

$\Gamma(\mathrm{n.m.})/\Gamma(\pi^-) \approx 0.15$ (from an experiment [20]),

$\Gamma(\pi^0)/\Gamma(\pi^-) \approx 0.16$ (calculated by Dalitz [21]),

$\Gamma(\pi^-\,{}^{4}\mathrm{He})/\Gamma(\pi^-) \approx 0.89$ (from experiments, see Table 4),

where $\Gamma(\mathrm{n.m.})$, $\Gamma(\pi^-)$, and $\Gamma(\pi^0)$ stand for non-mesic, π^--mesic, and π^0-mesic decay rates, respectively. The branching ratio $\mathrm{BR}(\pi^-\,{}^{4}\mathrm{He})$ is obtained as :

$$\mathrm{BR}(\pi^-\,{}^{4}\mathrm{He}) = \frac{\Gamma(\pi^-\,{}^{4}\mathrm{He})}{\Gamma(\mathrm{n.m.}) + \Gamma(\pi^-) + \Gamma(\pi^0)} \approx 0.7.$$

REFERENCES

1. T. Yamazaki *et al.*, Phys. Lett. 144B (1984) 177.
2. R. Bertini *et al.*, Phys. Lett. 90B (1980) 375.
3. H. Piekarz *et al.*, Phys. Lett. 110B (1982) 428.
4. R. Bertini *et al.*, Phys. Lett. 136B (1984) 29.
5. R. Bertini *et al.*, Phys. Lett. 158B (1985) 19.
6. A. Matsuyama and K. Yazaki, Contributed paper M25 to the 10th Int. Conf. on Particles and Nuclei, Heidelberg (1984); to be published.
7. A. Gal and L. Klieb, Phys. Rev. C34 (1986) 956.
8. O. Morimatsu and K. Yazaki, to be published; O. Morimatsu, thesis, Univ. of Tokyo, 1986.
9. T. Yamazaki *et al.*, Phys. Rev. Lett. 54 (1985) 102.
10. M. Iwasaki, Thesis, Univ. of Tokyo, 1987.
11. R.S. Hayano, Proceedings of Int. Conf. on Particle and Nuclei, Kyoto (1987).
12. M. Kohno *et al.*, to be published.
13. C. Vander Velde-Wilquet *et al.*, Nuovo Cimento 39A (1977) 537.
14. M.A. Faessler *et al.*, Phys. Lett. 46B (1973) 468.
15. W. Brückner *et al.*, Phys. Lett. 79B (1978) 157.
16. R.H. Dalitz *et al.*, Nucl. Phys. A450 (1986) 311c.
17. M.Juric *et al.*, Nucl. Phys. B52 (1973) 1.
18. G. Bohm *et al.*, Nucl. Phys. B4 (1968) 511.
19. T. Ishikawa *et al.*, KEK 12GeV PS Proposal, (1987).
20. R.H. Dalitz, Proceedings of Int. Conf. on Hyperfragments St.Cergue (1964), CERN report 64-1, p.147.
21. R.H. Dalitz and L.Liu, Phys. Rev. 5 (1959) 1312.